Synthesis of New Polycyclic Oxazol-2-one Derivatives by a Tandem [4 + 2] Cycloaddition/Cyclopentannulation/1,5-Sigmatropic Rearrangement Process of Fischer (Arylalkynyl)(alkoxy)carbenes and *exo*-2-Oxazolidinone Dienes

Leonor Reyes,[†] Humberto Mendoza,[†] Miguel Angel Vázquez,[‡] Fernando Ortega-Jiménez,[§] Aydeé Fuentes-Benítes,[||] María Inés Flores-Conde,[†] Hugo Jiménez-Vázquez,[†] René Miranda,[§] Joaquín Tamariz,[†] and Francisco Delgado*[,†]

Departamento de Química Orgánica, Escuela Nacional de Ciencias Biológicas-IPN, Prol. Carpio y Plan de Ayala, 11340 México, D.F., México, Departamento de Ciencias Químicas, Facultad de Estudios Superiores Cuautitlán-UNAM, Campo 1, Avenida 1ro. de Mayo s/n, Cuautitlán Izcalli, Estado de México 54740, México, Facultad de Química, Universidad de Guanajuato, Noria Alta, s/n, Guanajuato Gto. 36050, México, and Departamento de Química Orgánica, Facultad de Química, Universidad Autónoma del Estado de México, Paseo Colón/Paseo Tollocan s/n, Toluca, Estado de México 50000, México

Received March 15, 2008

An efficient and simple synthesis of highly substituted 9-ethoxy-3-phenyl-3*H*-fluorene[3,2-*d*]oxazol-2-(4*H*,9*H*,10*H*)-one derivatives **10a**−**f** by a tandem [4 + 2] cycloaddition/cyclopentannulation process of Fischer (arylethynyl)(ethoxy)carbene complexes $(CO)_5M{=}C(C{\equiv}CC_6H_4\text{-}R)OCH_2CH_3$ (**1a**, M = Cr, R = H; **1b**, M = Cr, R = *p*-CH_3; **1c**, M = Cr, R = *p*-OCH_3; **1d**, M = W, R = H; **1e**, M = W, R = *p*-CH_3; **1f**, M = W, R = *p*-OCH_3) with *exo*-2-oxazolidinone dienes **7a**−**d** is described. A study of reactivity as well as regio- and stereoselectivity in a tandem process of the Fischer carbene complexes **1** with the *exo*-heterocyclic dienes **7** was carried out. The cycloadditions were found to be highly regioselective, favoring the *para* cycloadducts, and highly stereoselective, giving the *trans* diastereoisomers. The stereochemical assignment of the cycloadducts was supported by NOE measurements, and the derivatives **10b**,**c**,**e** were further characterized by single crystal X-ray diffraction. A rationalization of the regioselectivity was carried out through an FMO analysis of the energies and coefficients for the most stable conformations of carbenes **1a**,**d** and for diene **7a**, showing a stronger interaction for the observed *para* cycloadduct than for the *meta* regioisomer. The aromatization of cycloadducts **10a**−**f** with HCl and DDQ is also reported.

Introduction

Cycloaddition processes via organometallic compounds are essential in organic synthesis for the construction of heterocyclic and carbocyclic compounds.[1] In particular, Fischer carbene complexes of group 6 are of interest, due to the fact that these organometallic compounds offer the opportunity to access heterocyclic and carbocyclic rings, not easily available through conventional routes. In this context, α,β-unsaturated carbene complexes involving the Dötz [3 + 2 +1][2] and Diels−Alder [4 + 2][3] cycloadditions are particularly important. Among these processes, the Diels−Alder cycloaddition of alkynylcarbene complexes with dienes, which often involves cascade reactions, has proven a useful route for the synthesis of a wide variety of polycyclic compounds from simple synthetic building blocks.[1g,3] It is well-known that (arylalkynyl)carbene complexes can be employed as dienophiles in Diels−Alder reactions. The resultant *cis*-1,3,5-metallahexatriene adducts can react further to form cyclopentadienes spontaneously, thermally, or photolytically to produce phenol derivatives.[4] One unique feature of Fischer carbene complex chemistry is the seemingly minor but extraordinary variation in the substrates, as well as the remarkable

* To whom correspondence should be addressed. E-mail: fdelgado@woodward.encb.ipn.mx.
[†] Escuela Nacional de Ciencias Biológicas-IPN.
[‡] Universidad de Guanajuato.
[§] Facultad de Estudios Superiores Cuautitlán-UNAM.
[||] Universidad Autónoma del Estado de México.

(1) (a) Fischer, E. O.; Maasböl, A. *Angew. Chem., Int. Ed. Engl.* **1964**, *3*, 580–581. (b) Herndon, J. W. *Coord. Chem. Rev.* **2007**, *251*, 1158–1258. (c) Barluenga, J.; Santamaría, J.; Tomás, M. *Chem. Rev.* **2004**, *104*, 2259–2283. (d) Yamamoto, Y.; Hayashi, H. *Tetrahedron* **2007**, *63*, 10149–10160. (e) Gómez-Gallego, M.; Mancheño, M. J.; Sierra, M. A. *Acc. Chem. Res.* **2005**, *38*, 44–53. (f) Harvey, D. F.; Sigano, D. M. *Chem. Rev.* **1996**, *96*, 271–288. (g) Barluenga, J.; Fernández-Rodríguez, M. A.; Aguilar, E. *J. Organomet. Chem.* **2005**, *690*, 539–587. (h) Barluenga, J.; Martínez, S.; Suárez-Sobrino, A. L.; Tomás, M. *Org. Lett.* **2008**, *10*, 677–679. (i) Bertrand, G., *Carbene Chemistry: From Fleeting Intermediates to Powerful Reagents*; Marcel Dekker: New York, 2002.

(2) (a) Dötz, K. H.; Tomuschat, P. *Chem. Soc. Rev.* **1999**, *28*, 187–198. (b) Lian, Y.; Wulff, W. D. *J. Am. Chem. Soc.* **2005**, *127*, 17162–17163. (c) Gopalsamuthiram, V.; Wulff, W. D. *J. Am. Chem. Soc.* **2004**, *126*, 13936–13937. (d) Dötz, K. H. *Metal Carbenes in Organic Synthesis (Topics in Organometallic Chemistry)*; Springer-Verlag: New York, 2004.

(3) (a) Wulff, W. D.; Yang, D. C. *J. Am. Chem. Soc.* **1983**, *105*, 6726–6727. (b) Vázquez, M. A.; Cessa, L.; Vega, J. L.; Miranda, R.; Jiménez-Vázquez, H. A.; Tamariz, J.; Delgado, F. *Organometallics* **2004**, *23*, 1918–1927. (c) Barluenga, J.; Aznar, F.; Palomero, M. A. *J. Org. Chem.* **2003**, *68*, 537–544. (d) Wu, H.-P.; Aumann, R.; Fröhlich, R.; Wibbeling, B. *Eur. J. Org. Chem.* **2000**, 1183–1192. (e) Wu, H.-P.; Aumann, R.; Fröhlich, R.; Saarenketo, P. *Chem. Eur. J.* **2001**, *7*, 700–710.

(4) (a) Merlic, C. A.; Xu, D.; Gladstone, B. G. *J. Org. Chem.* **1993**, *58*, 538–545. (b) Aumann, R. *Eur. J. Org. Chem.* **2000**, *1*, 7–31. (c) Vázquez, M. A.; Reyes, L.; Miranda, R.; García, J. J.; Jiménez-Vázquez, H. A.; Tamariz, J.; Delgado, F. *Organometallics* **2005**, *24*, 3413–3421. (d) Barluenga, J.; Fernández-Rodríguez, M. A.; Andina, F.; Aguilar, E. *J. Am. Chem. Soc.* **2002**, *124*, 10978–10979. (e) Barluenga, J.; Aznar, F.; Angel Palomero, M. A.; Barluenga, S. *Org. Lett.* **1999**, *1*, 541–543.

10.1021/om8002416 CCC: $40.75
Publication on Web 08/13/2008

Scheme 1

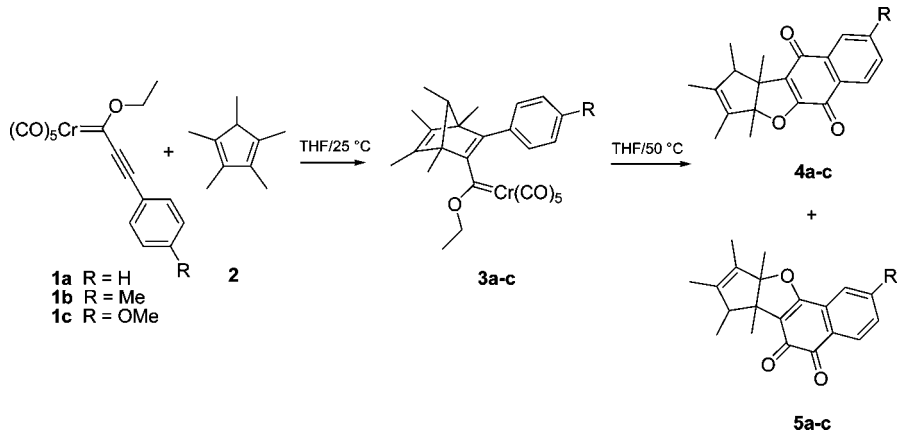

Scheme 2

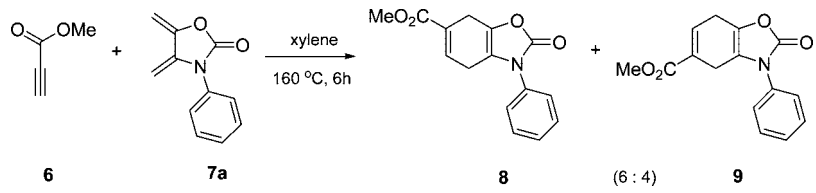

conditions that change the course of the reaction and the structure of its product.

We have recently reported that (arylethynyl)(ethoxy)carbene complexes of chromium of metals of group 6 (**1**) react with 1,2,3,4,5-pentamethyl-1,3-cyclopentadiene (**2**) under thermal conditions, leading to the formation of 1,2- and 1,4-naphthofurandiones **4** and **5** through a tandem Diels−Alder/benzannulation/rearrangement process.[4c] The *cis*-1,3,5-metallahexatriene (**3**) formed from the initial Diels−Alder reaction was involved to form the benzannulation product, and the subsequent rearrangement of the latter formed naphthofurandiones **4** and **5** (Scheme 1).

On the other hand, cyclic 1,3-dienes have been widely used for evaluating the reactivity, regio- and stereoselectivity, and π-facial selectivity in Diels−Alder cycloadditions.[5] The preparation and study of *exo*-heterocyclic dienes have been the subject of numerous investigations.[6] In addition, we have reported a one-pot synthesis of the novel *N*-substituted 4,5-dimethylene-*exo*-2-oxazolidinones,[7] and their application in the total synthesis of natural carbazoles.[8] However, the thermal Diels−Alder cycloaddition of the *exo*-2-oxazolidinone diene **7a** with methyl propiolate **6** yields relatively low regioselectivity (6:4 *para*:*meta*) (Scheme 2).[7b] This was improved by carrying out the reaction in polar solvents.[8b]

With the aim of evaluating the reactivity and selectivity in the Diels−Alder reaction of the Fischer carbene complexes **1** with diene **7** and the possible subsequent annulation of the resulting adducts, we herein report a convenient and versatile synthesis of substituted 9-ethoxy-3-phenyl-3*H*-fluorene[3,2-*d*]oxazol-2-(4*H*,9*H*,10*H*)-one derivatives **10a**−**f** in a highly regio- and stereoselective tandem process, starting from the Fischer (arylethynyl)(ethoxy)carbene complexes (Cr and W) **1a**−**f** and *exo*-2-oxazolidinone dienes **7a**−**d**. In addition, we evaluated the effect of the substituents in the carbene complexes and in the *exo*-heterocyclic dienes on the reactivity as well as regio- and stereoselectivity of the tandem process. Finally, the aromatization of compounds **10a**−**f** was carried out to access the skeleton of the 9-ethoxy-3-phenyl-3*H*-fluorene[3,2-*d*]oxazol-2(9*H*)-one and 3-phenyl-3*H*-fluorene[3,2-*d*]oxazol-2(9*H*)-one compounds (**14** and **15**, respectively).

Results and Discussion

Tandem Reactions of Complexes 1 with Dienes 7. The reactions between the (arylethynyl)(ethoxy)carbene complexes **1a**−**f** and *N*-substituted *exo*-2-oxazolidinone dienes **7a**−**d** were evaluated in terms of reactivity and selectivity in Diels−Alder reactions. Thus, a mixture of **1a** (1.0 mol equiv) and **7a** (1.0 mol equiv) was reacted in THF at 50 °C. Only one product was obtained, judging from the thin-layer chromatographic and ^{1}H NMR (300 MHz) analysis of the crude reaction mixture.

The isolated compound, surprisingly, was not the expected Diels−Alder cycloadduct. Instead, compound **10a** was obtained in 40% yield (Table 1, entry 1). This result proved that (arylethynyl)(ethoxy)carbene **1a** undergoes a cascade process with the *exo*-2-oxazolidinone diene **7a** under thermal conditions. We were pleased to discover that the reaction proceeded with complete regiocontrol, producing cycloadduct **10a** as the only regioisomer. It is likely that steric and electronic effects at the transition state for the approach of **1a** as dienophile with the

(5) Fringuelli, F.; Taticchi, A. *Dienes in the Diels-Alder Reaction*; Wiley: New York, 1990; pp 125−147.

(6) (a) Toda, F.; Garratt, P. *Chem. Rev.* **1992**, *92*, 1685–1705. (b) Cava, M. P.; Mitchell, M. J. *Cyclobutadiene and Related Compounds*; Academic Press: New York, 1967. (c) Chou, C.-H.; Trahanovsky, W. S. *J. Org. Chem.* **1995**, *60*, 5449–5451.

(7) (a) Hernández, R.; Sánchez, J. M.; Gómez, A.; Trujillo, G.; Aboytes, R.; Zepeda, G.; Bates, R. W.; Tamariz, J. *Heterocycles* **1993**, *36*, 1951. (b) Mandal, A.; Gómez, A.; Trujillo, G.; Méndez, F.; Jiménez, H.; Rosales, M.; Martínez, R.; Delgado, F.; Tamariz, J. *J. Org. Chem.* **1997**, *62*, 4105–4115. (c) Benavides, A.; Martínez, R.; Jiménez-Vázquez, H. A.; Delgado, F.; Tamariz, J. *Heterocycles* **2001**, *55*, 469–485. (d) Martínez, R.; Jiménez-Vázquez, H.; Delgado, F.; Tamariz, J. *Tetrahedron* **2003**, *59*, 481–492. (e) Fuentes, A.; Martínez-Palou, R.; Jiménez-Vázquez, H. A.; Delgado, F.; Reyes, A.; Tamariz, J. *Monatsh. Chem.* **2005**, *136*, 177–192.

(8) (a) Benavides, A.; Peralta, J.; Delgado, F.; Tamariz, J. *Synthesis* **2004**, 2499–2504. (b) Zempoalteca, A.; Tamariz, J. *Heterocycles* **2002**, *57*, 259–267. (c) Mandal, A. B.; Delgado, F.; Tamariz, J. *Synlett.* **1998**, 87–89. (d) Bernal, P.; Benavides, A.; Bautista, R.; Tamariz, J. *Synthesis* **2007**, 1943–1948. (e) Bernal, P.; Tamariz, J. *Helv. Chim. Acta* **2007**, *90*, 1449–1454.

Table 1. Tandem Reactions of Carbene Complexes 1a−f with Dienes 7a−c[a,b]

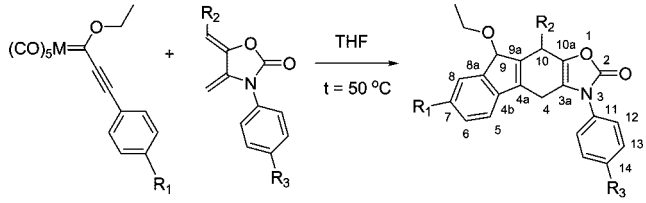

1a M = Cr R_1 = H **7a** R_2 = H R_3 = H
1b M = Cr R_1 = CH_3 **7b** R_2 = CH_3 R_3 = H
1c M = Cr R_1 = OCH_3 **7c** R_2 = Et R_3 = H
1d M = W R_1 = H **7d** R_2 = CH_3 R_3 = Cl
1e M = W R_1 = CH_3
1f M = W R_1 = OCH_3

entry	carbene	diene	time (h)	product	yield (%)[c]
1	**1a**	**7a**	8	**10a**	40
2	**1a**	**7b**	6	**10b**	45
3	**1a**	**7c**	8	**10c**	70
4	**1a**	**7d**	6	**10d**	60
5	**1b**	**7b**	8	**10e**	65
6	**1c**	**7b**	8	**10f**	60
7	**1d**	**7b**	10	**10b**	55
8	**1e**	**7b**	11	**10e**	40
9	**1f**	**7b**	13	**10f**	45

[a] All the reactions were carried out with 1 mol equiv of **1** and **7**. [b] All the reactions were carried out at 50 °C. [c] After column chromatography.

Scheme 3

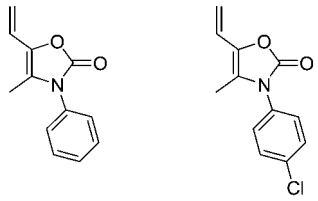

11a **11b**

bulky and electron-withdrawing pentacarbonyl(carbene)chromium group are responsible for the high regioselectivity observed.

It has been reported that methyl propiolate (**6**) reacts with **1a** after 6 h at 160 °C, to give a mixture of the corresponding *para* and *meta* cycloadducts in a 6:4 ratio (Scheme 2).[7b] In contrast, cycloaddition with the (arylethynyl)(ethoxy)carbene complex **1a** was carried out at 50 °C (8 h), furnishing only the *para* regioisomer. This result indicates that complex **1a** is more reactive and regioselective that dienophile **6**.

The structural elucidation of product **10a** was made on the basis of its spectroscopic data. The infrared spectrum displays characteristic absorptions at 1763 and 1714 cm^{-1}, indicating the presence of the fluorenyloxazol-2-(4*H*,9*H*,10*H*)-one core. The ^1H NMR spectrum of **10a** shows the presence of nine contiguous protons in the aromatic region, with signals in the range of 7.55−7.10 ppm (H-5, H-6, H-7, H-8, H-12, H-13, and H-14). At 5.07 ppm, a singlet was found to correspond to one proton (H-9); at 3.55−3.28, a multiple signal was found to correspond to six protons (H-4, H-10, and OCH_2CH_3). The ^{13}C NMR spectrum displayed a signal at 155.2 ppm (C-2) due to a carbonyl group, 14 signals at 143.8−118.3 ppm for vinyl and aromatic carbons, and 5 signals at 82.7, 60.9, 22.6, 21.0, and 15.6 ppm for sp^3 carbon atoms. Furthermore, the HMBC spectrum of **10a** showed two- and three-bond C−H long-range correlations between the protons at 3.50 ppm and the carbon atoms at 137.4, 133.4, and 118.7 ppm, in agreement with the presence of a 3*H*-fluorene[3,2-*d*]oxazol-2-(4*H*,9*H*,10*H*)-one system.

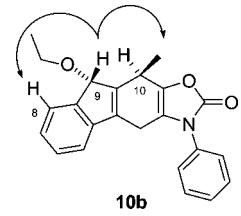

Figure 1. NOE observed upon irradiation of proton H-9 in adduct **10b**.

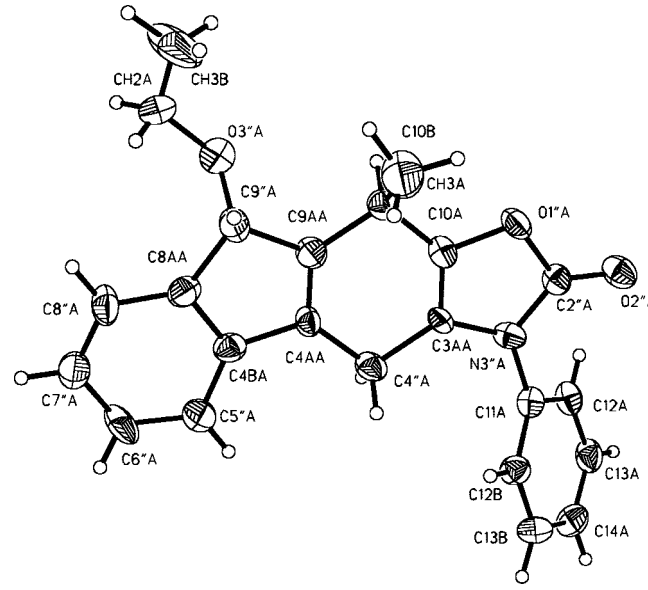

Figure 2. Molecular structure of **10b** with thermal ellipsoids at the 30% probability level.

In order to evaluate the effect of the substituent in the *exo*-2-oxazolidinone dienes on the reactivity and selectivity in the course of the tandem reactions, dienes **7b−d**, bearing a methyl or an ethyl group in the double bond, were added under identical conditions to alkynylcarbene complexes **1a−f**. These reactions furnished the 9-ethoxy-3-phenyl-3*H*-fluorene[3,2-*d*]oxazol-2-(4*H*,9*H*,10*H*)-one cycloadducts **10b−f** (Table 1, entries 2−9), and as a byproduct the dienes **11a**,**b** were formed by the [1,5]-sigmatropic rearrangement of dienes **7b**,**d**, respectively (Scheme 3).[7b]

The new fluorenyloxazolones **10b−f** were isolated as solids. Their ^1H and ^{13}C NMR spectra were consistent with the presence of the 3*H*-fluorene[3,2-*d*]oxazol-2-(4*H*,9*H*,10*H*)-one skeleton. The stereochemical assignment of **10b** was supported by NOE experiments, where the signals of protons H-8 (7.54 ppm) and CH_3 (1.53 ppm) were enhanced when the H-9 proton (5.20 ppm) was irradiated (Figure 1). Consequently, the disposition between the methyl group at C-10 and the ethoxy group at C-9 is anti, and the regioisomer obtained is the *para* cycloadduct.

The regiochemistry and stereochemistry for cycloadducts **10b**,**c** were unambiguously determined by X-ray crystallography (Figures 2 and 3).

As shown in Table 1, among the *exo*-2-oxazolidinone dienes examined, the ethyl-substituted *exo*-heterocyclic diene **7c** was the most efficient, as evidenced by the fact that the yield was the best, giving a single regioisomer and stereoisomer, **10c** (Table 1, entry 3). Although *exo*-heterocyclic dienes **7b**,**d** showed a reactivity higher than that observed for diene **7c** (Table 1, entries 2 and 4), the yields were lower. In contrast, a similar reactivity was observed for the Diels−Alder addition between

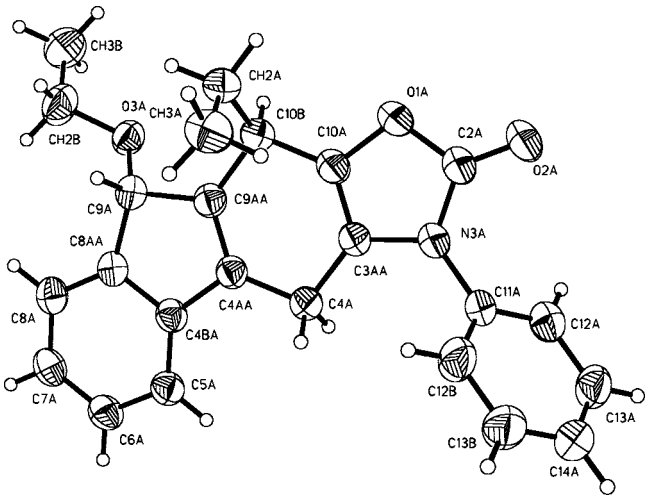

Figure 3. Molecular structure of **10c** with thermal ellipsoids at the 30% probability level.

the methyl- and ethyl-substituted dienes with methyl propiolate (**6**).[7e] However, the regioselectivity for the latter dienophile was lower in comparison with carbene complexes **1a**−**f**, as shown by the mixture of the *para* and *meta* (6:4) regiosiomers obtained. It is noteworthy that the change in the metal atom of the (arylethynyl)(ethoxy)carbene complexes seems to affect the reactivity, as the relative rate is reduced when chromium is replaced by tungsten (Table 1, entries 7−9). Nevertheless, the regio- and stereoselectivity observed in the corresponding adducts does not seem to be influenced by a change of the metal atom.

Kinetic measurements made by Wulff, with alkenylcarbenes in Diels−Alder reactions in the presence of isoprene, show that the tungsten carbenes are slightly more reactive than the chromium carbenes.[9] Our molecular orbital calculations also support this trend (vide infra). It is likely that the shorter reaction times recorded for the chromium carbene **1a**, with respect to those for the tungsten carbene **1d**, are due to the fact that the former carbene was less stable under the reaction conditions, as observed by ^{1}H NMR monitoring of samples of both carbenes. Since the determination of the reaction time was based on the consumption of the starting carbene, the faster decomposition of the chromium carbenes would lead to an incorrect evaluation of the reactivity.

These results proved that the (arylethynyl)(ethoxy)carbene complexes **1a**−**f** undergo cascade reactions with the *exo*-2-oxazolidinone dienes **7a**−**d** under thermal conditions. The mechanism of the reaction is outlined in Scheme 4. Initially, the regioselective [4 + 2] cycloaddition of complexes **1a**−**f** to dienes **7a**−**d** produces the unstable *cis*-1,3,5-metallahexatriene **I**, which undergoes a subsequent selective intramolecular electrocyclic ring closure, furnishing intermediate **II**. Preferential cyclopentannulation rather than benzannulation is illustrated by the absence of any benzene-derived product in the intramolecular reaction of **I** and is consistent with the known behavior of *cis*-1,3,5-metallahexatriene **I** under thermal conditions.[10] Then, intermediate **II** undergoes a 1,5-sigmatropic rearrangement and successive reductive elimination of the metallic fragment, leading to the formation of compounds **10a**−**f**.

In our opinion, the unstable *cis*-1,3,5-metallahexatriene **I**, formed from diene **7** and initial arylethynylcarbene complex **1**, is the key intermediate in the above tandem process. In an effort to isolate intermediate **I**, which is suspected of being the precursor of fluorenyloxazolone **10**, carbene complexes **1a**,**d** were treated with diene **7b** at −78 °C at room temperature for 24 h. However, they failed to give the [4 + 2] adducts, providing only a ∼40% yield of the product of oxidation of starting carbene complexes, a ∼15% yield of diene **11a**, and less than ∼20% of the cycloadduct **10b**, in accordance with the ^{1}H NMR (300 MHz) analysis of the crude reaction mixtures. With the same purpose, we prepared the (propylethynyl)(ethoxy)carbene complex **12**[11] and submitted it under the above conditions to the reaction with the methyl-substituted *exo*-heterocyclic diene **7b** (Scheme 5). After workup, only the [4 + 2] carbene complex cycloadduct **13** was obtained in fairly good yield (55%). It is noteworthy that the ^{1}H NMR analysis of the crude mixture did not show evidence of the presence of any other isomer; hence, the cycloaddition reaction was exclusively *para* regioselective.

The new 5-butyl-7-methyl-2-oxo-3-phenyl-2,3,4,7-tetrahydrobenzo[*d*]oxazole-6-ethoxymethylene pentacarbonyl complex **13** was isolated as an orange solid. Its ^{1}H and ^{13}C NMR spectra were consistent with the tetrahydrobenzo[*d*]oxazole skeleton, with the presence of a pentacarbonyl ethoxycarbene fragment, as well as alkyl and aryl groups. Thus, the ^{1}H NMR spectrum of **13** showed the presence of a monosubstituted benzene ring, with multiple signals attributed to protons H-10 at 7.51−7.46 ppm and to protons H-9 and H-11 at 7.39−7.36 ppm. At 5.00−4.94 and 4.17−4.01 ppm, two multiplets were found integrating for two protons (OCH_2CH_3) and one proton (H-7). In addition, two doublets, three triplets, and one quintuplet were observed at 3.00, 1.51, 1.85, 1.62, 0.95, and 1.43 ppm for H-4, H-15, H-12, OCH_2CH_3, H-14, and H-13 protons, respectively. In the ^{13}C NMR spectrum, the signal due to $C_{carbenic}$ appeared at 331.8 ppm, the signals of two nonequivalent CO groups at 202.8 and 196.8, and the signal for C-2 at 154.7 ppm. Furthermore, the HMBC spectrum of **13** showed two- and three-bond C−H long-range correlations between the protons at 3.00 ppm (H-4) and the carbon atoms at 150.9 (C-5), 135.1 (C-7a), 121.3 (C-6), and 117.3 ppm (C-3a). In the NOE experiments, the signals of protons H-9 (7.36 ppm), H-12 (1.86 ppm), and H-13 (1.44 ppm) were enhanced when the H-4 protons (3.00 ppm) were irradiated (Figure 4), in agreement with the presence of a tetrahydrobenzo[*d*]oxazole-6-ethoxymethylene pentacarbonyl complex system.

Unlike the reaction between **7b** and **1**, which generates the tandem reaction, the reaction of diene **7b** with carbene complex **12**, which does not contain an additional γ-carbon−δ-carbon double bond or a benzene ring to promote the annulation, afforded the expected Diels−Alder cyloadduct, **13**. These results suggest that the unstable complex **I** may be considered as a precursor in the formation of fluorenyloxazolone **10** (Scheme 4).

Evaluation of the Reactivity and Selectivity of the Diels−Alder Cycloadditions by FMO Analysis. The reactivity and regioselectivity of dienes **7** in Diels−Alder cycloadditions has been accounted for satisfactorily by FMO theory with a series of dienophiles.[7b,e] Therefore, this model should also be useful to correlate the energies and coefficients of the frontier molecular orbitals of diene **7a** with those of dienophiles **1a**,**d**.

(9) Wulff, W. D.; Bauta, W. E.; Kaesler, R. W.; Lankford, P. J.; Miller, R. A.; Murray, C. K.; Yang, D. C. *J. Am. Chem. Soc.* **1990**, *112*, 3642–3659.

(10) (a) Dötz, K. H. *J. Organomet. Chem.* **1977**, *140*, 177–186. (b) Wulff, W. D.; Tang, P.-C.; Chan, K.-S.; McCallum, J. S.; Yang, D. C.; Gilbertson, S. R. *Tetrahedron* **1985**, *41*, 5813–5832. (c) Aumann, R.; Meyer, A. G.; Fröhlich, R. *Organometallics* **1996**, *15*, 5018–5027. (d) Barluenga, J.; Tomás, M.; Ballesteros, A.; Santamaría, J.; Suárez-Sobrino, A. *J. Org. Chem.* **1997**, *62*, 9229–9235.

(11) Duetsch, M.; Stein, F.; Lackmann, R.; Pohl, E.; Herbst-Irmer, R.; de Meijere, A. *Chem. Ber.* **1992**, *125*, 2051–2065.

Scheme 4

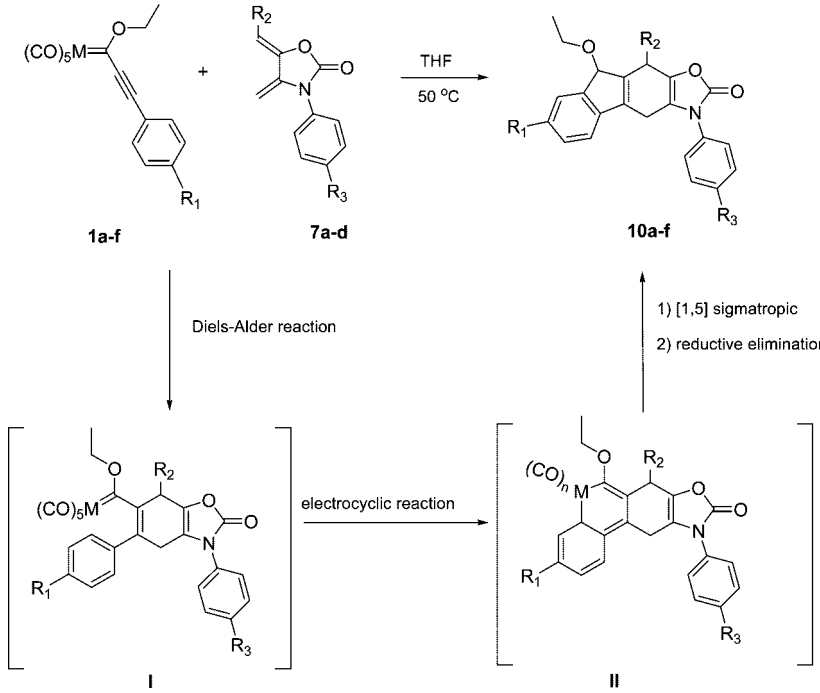

Scheme 5

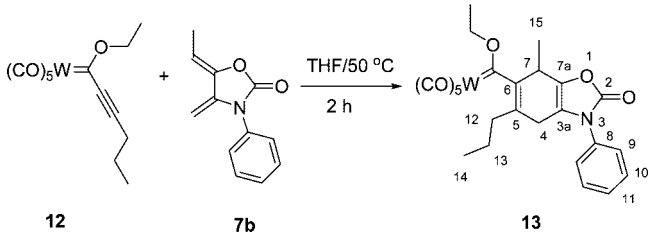

With the aim of comparing the reactivity and regioselectivity of the latter with the oxidized species, phenylethyl propiolate **14** was also calculated. Frontier orbitals of these cycloaddends were obtained from B3LYP/6-31G* calculations.[12] The structures of carbenes **1a**,**d** were fully optimized at the same level of theory, showing that the ethoxy group can adopt two distinct conformations, in accordance with other reports.[13] Thus, we carried out the corresponding geometry optimizations and frequency analysis on the anti and *syn* geometries. Table 2 summarizes the minimized energies obtained for these dienophiles. For the case of carbenes **1a**,**d**, the results show that the anti conformer is more stable than the *syn*, probably as a result of steric repulsion between the CH_2 fragment of the ethoxy group and the carbonyl ligands of the metal.[14] Consequently, the *syn* conformer is not planar. There is a relatively large deviation from planarity for the delocalized system formed by the phenyl ring, the triple bond, the carbenic carbon, and the oxygen and metal atoms (Figure 5). This conformation is

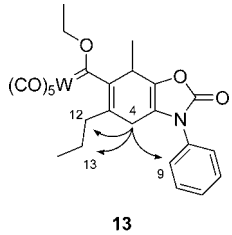

Figure 4. NOE observed upon irradiation of proton H-4 in adduct **13**.

Table 2. ZPE-Corrected Electronic (E_0, in au) and Relative (ΔE_0, in kcal/mol) Energies for the Anti and *syn* Conformers of 1a,d and 14

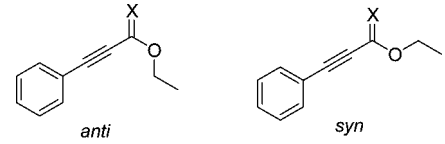

1a, X = $Cr(CO)_5$
1d, X = $W(CO)_5$
14, X = O

conformer		1a	1d	14
syn	E_0	−1 153.112 463	−1 134.681 445	−575.396 728
anti	E_0	−1 153.116 361	−1 134.683 829	−575.389 171
syn	ΔE_0	2.45	1.50	−4.74
anti	ΔE_0	0.00	0.00	0.00

essentially the same for both carbenes. A fully planar geometry was also calculated for the *syn* conformer, including two of the equatorial substituents of the metallic fragment in the same plane as the delocalized system. However, this turned out to be a transition state for the rotation of the $M(CO)_5$ fragment. On the other hand, the anti conformer is completely planar (Figure 5), a fact that further supports the idea that the deviation of planarity of the *syn* conformer is due to steric repulsion. In contrast, the corresponding *syn* and anti conformers for ester **14** were found to be completely planar, the former being the most stable (Table 2), as is usually seen in esters.[15]

Additional features of these conformers can be seen in Figure 5. Ratter than being completely linear, the triple bond is slightly

(12) Frisch, M. J.; Trucks, G. W.; Schlegel, H. B.; Gill, P. M. W.; Johnson, B. G.; Robb, M. A.; Cheeseman, J. R.; Keith, T.; Petersson, G. A.; Montgome, J. A.; Raghavachari, K., Al-Laham, M. A.; Zakrzewski, V. G.; Ortiz, J. V.; Foresman, J. B.; Cioslowski, J.; Stefanov, B. B.; Nanayakkara, A.; Challacombe, M.; Peng, C. Y.; Ayala, P. Y., Chen, W.; Wong, M. W.; Andres, J. L.; Replogle, E. S.; Gomperts, R.; Martin, R. L.; Fox, D. J.; Binkley, J. S.; Defrees, D. J.; Baker, J.; Stewart, J. P.; Head-Gordon, M.; Gonzalez, C.; Pople, J. A. Gaussian 94, Revision E.2; Gaussian, Inc., Pittsburgh, PA, 1995.

(13) (a) Fernández, I.; Cossío, F. P.; Arrieta, A.; Lecea, B.; Mancheño, M. J.; Sierra, M. A. *Organometallics* **2004**, *23*, 1065–1071. (b) Gu, K.; Yang, G.; Zhang, W.; Liu, X.; Yu, Z.; Han, X.; Bao, X. *J. Organomet. Chem.* **2006**, *691*, 1984–1992.

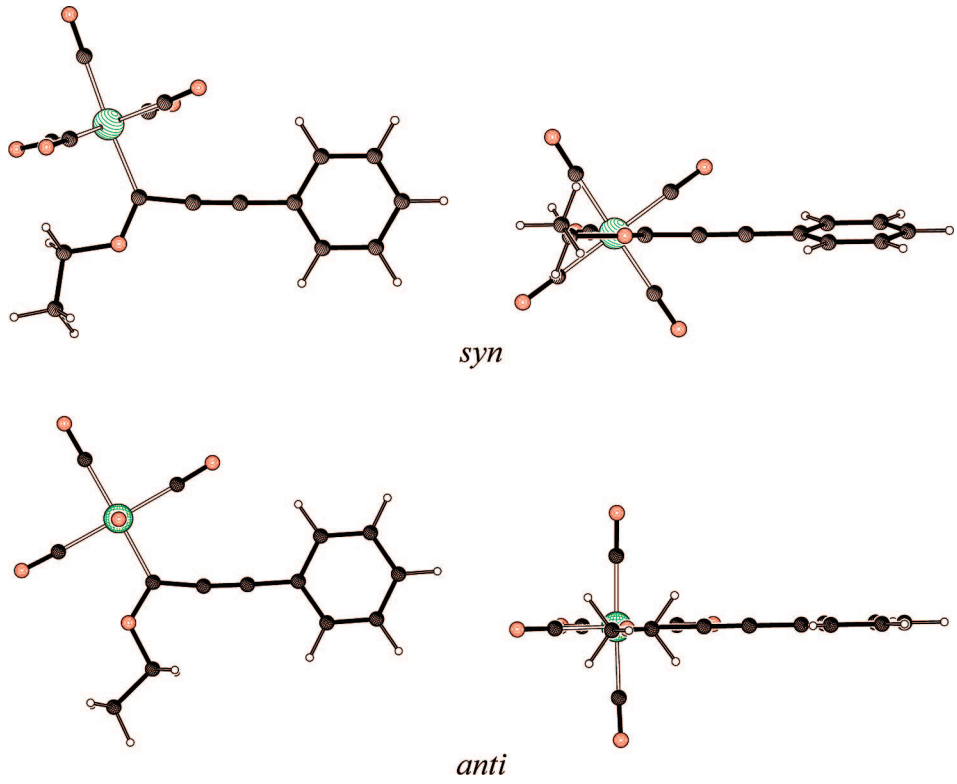

Figure 5. Two different views of the calculated geometries for the *syn* (top) and anti (bottom) conformers of the Cr carbene complex **1a**.

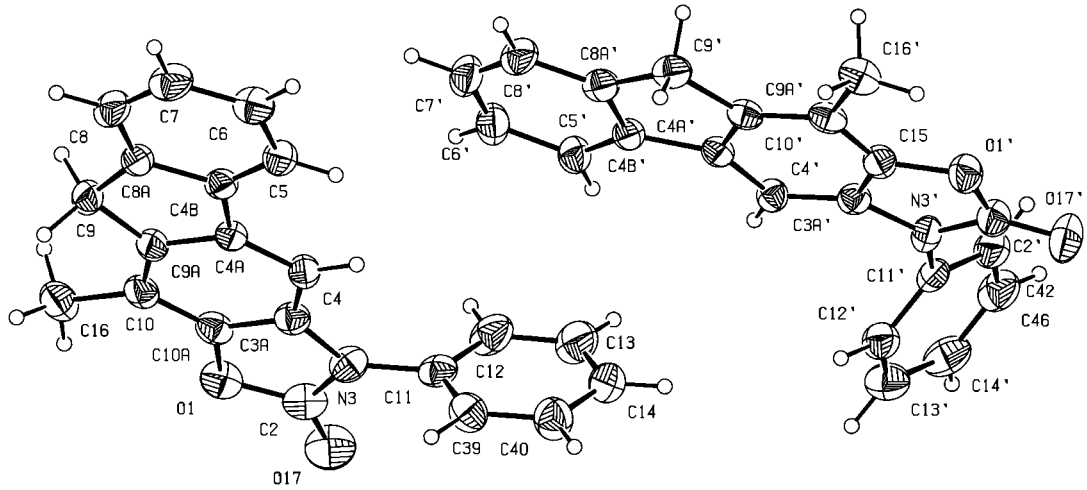

Figure 6. Molecular structure of **16b** with thermal ellipsoids at the 30% probability level.

bent, describing a curve. In particular, for the anti conformers, there seems to be a hydrogen bond between one of the *ortho* hydrogens of the phenyl ring and the nearest equatorial carbonyl oxygen (2.664 Å for the Cr complex), a fact that is likely to be responsible for the slightly greater bending of the triple bond. Even though a similar interaction could be proposed for the *syn* conformer, in this case the shortest CO···HC distance is 3.047 Å.

Table 3. Bond Lengths (Å) between the Metal and the Carbon Atoms in the Metallic Fragment of Carbene Complexes 1a,d[a]

	1a (Cr)		**1d** (W)	
bond	*syn*	anti	*syn*	anti
M=C	2.067	2.032	2.195	2.169
M−(CO)$_{cis}$	1.892	1.898	2.055	2.060
M−(CO)$_{trans}$	1.906	1.906	2.060	2.061

[a] The value shown for the M−(CO)$_{trans}$ bond length corresponds to the average M−C bond length for all four equatorial CO ligands.

In addition to the two conformers already mentioned, we calculated two more conformers with the phenyl ring perpendicular to those shown in Figure 5. This was done because Han and co-workers, in a theoretical study of W carbene **1c** (carried out at a different level of theory), reported conformers with the phenyl ring in this geometry.[13b] However, in our calculations

(14) It has been reported that for (alkoxy)carbene complexes, substituents other than an alkynyl group make the *syn* conformer more stable than the anti.[13a]

(15) See for example: (a) Wang, X.; Houk, K. N. *J. Am. Chem. Soc.* **1988**, *110*, 1870–1872. (b) Wiberg, K. B.; Laidig, K. B. *J. Am. Chem. Soc.* **1988**, *110*, 1872–1874. (c) Wiberg, K. B.; Laidig, K. B. *J. Am. Chem. Soc.* **1987**, *109*, 5935–5943. (d) Blom, C. E.; Günthard, H. H. *Chem. Phys. Lett.* **1981**, *84*, 267–271.

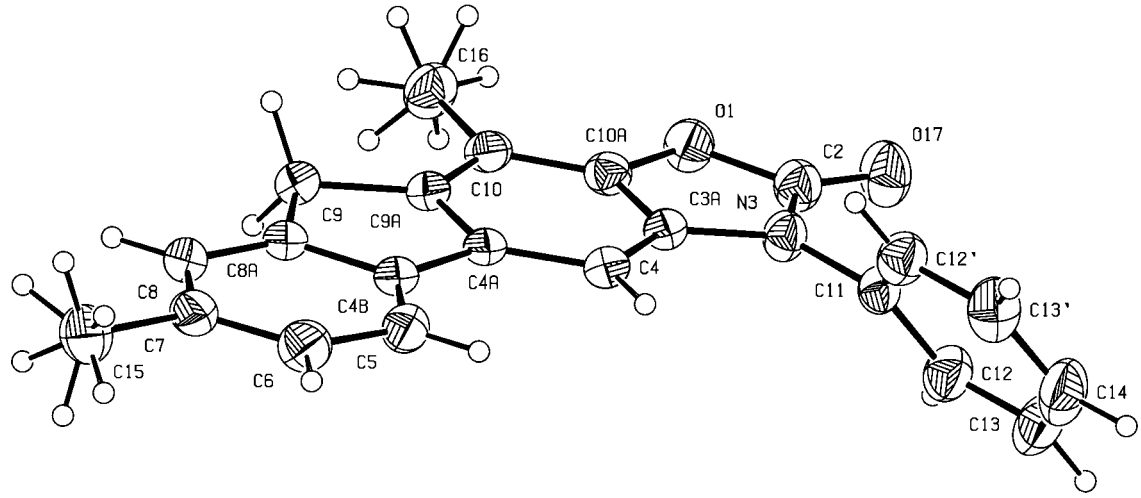

Figure 7. Molecular structure of **16e** with thermal ellipsoids at the 30% probability level.

Table 4. Calculated FMO Energies (eV) for Dienophiles 1a,d and 14 and Diene 7a

	1a (Cr)		**1d** (W)		**14**		
orbital[a]	*syn*	anti	*syn*	anti	*syn*	anti	**7a**
HOMO	−6.0257	−5.8698	−6.0051	−5.8608	−6.6067	−6.7624	−6.0249
LUMO	−2.6308	−2.7334	−2.7312	−2.8110	−1.6425	−1.7968	−1.2164

[a] For carbenes **1a**,**d**, the HOMO energy shown actually corresponds to the energy of the HOMO-1 orbital.

Table 5. Calculated HOMO−LUMO Energy Gaps (eV) for the Cycloaddition of Diene 7a to the *syn* or Anti Conformers of Dienophiles 1 or 14

	1a (Cr)		**1d** (W)		**14**	
gap[a]	*syn*	anti	*syn*	anti	*syn*	anti
$\Delta E(L_d-H_D)$	3.3941	3.2915	3.2937	3.2140	4.3824	4.2281
$\Delta E(L_D-H_d)$	4.8094	4.6535	4.7887	4.6445	5.3903	5.5460
$\Delta\Delta E$	1.4153	1.3619	1.4950	1.4305	1.0079	1.3179

[a] Legend: L = LUMO; H = HOMO; D = diene; d = dienophile; $\Delta\Delta E = \Delta E(L_d-H_D) - \Delta E(L_D-H_d)$.

these conformers turned out to be saddle points; thus, they were not considered any further.

The energy differences between the two conformers in compounds **1a**,**d** can be correlated to the M═C bond lengths, when the same conformers are compared (all *syn* or all anti), and thus to the degree of steric repulsion between the alkoxy group and the equatorial carbonyl ligands in the *syn* conformers; these distances are shown in Table 3. The Cr carbene complex, with the shortest M═C bond length, leads to the least stable *syn* conformer. In this respect the W complex follows, with the longest M═C bond length. Furthermore, the M═C bond length is slightly shorter for the anti conformers, supporting the idea of a smaller steric interaction between the alkoxy group and the metallic fragment.

For the FMO study of the dienophiles **1a**,**d** and **14**, the frontier orbitals expected to be involved in the cycloaddition reaction were located by visual inspection. For the carbenes, the corresponding HOMO orbital turned out to be HOMO-1. The energies of these orbitals for both *syn* and anti conformers are found in Table 4, as are those of ester **14**. For diene **7a**, the energies correspond to the molecular orbitals of the single conformer, which have been previously reported.[7b] The energy of the LUMO orbitals of the carbenes is lower than for **14**, with the energy being slightly lower (about 0.1 eV) in the anti conformers for all dienophiles. In addition, when the orbitals in the same conformers are compared, the stability of the LUMOs in the carbenes follows the trend Cr < W.

Table 6. Calculated Atomic Orbital Coefficients for the LUMOs of 1a,c and 14 and the HOMO of 7a[a]

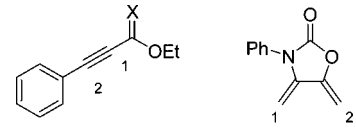

1a, X = $Cr(CO)_5$
1d, X = $W(CO)_5$
14, X = O

7a

coeff[b]	**1a** (Cr, anti)	**1d** (W, anti)	**14** (*syn*)	**7a**
c_1	−0.1240	−0.1117	−0.2167	0.3449
c_2	0.2910	0.2861	0.2426	−0.2403
Δc[c]	0.1670	0.1744	0.0259	0.1045

[a] Only the values corresponding to the most stable conformers are shown. [b] These values refer to the p_z coefficients numbered as shown in the structures; the p_z' coefficient values follow a similar trend. [c] $\Delta c = |c_2 - c_1|$.

Scheme 6

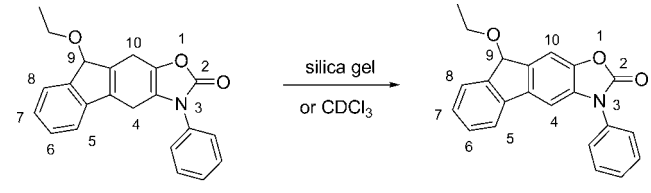

10a **15a**

Table 5 shows the LUMO−HOMO energy gaps calculated with the orbital energies in Table 4. It is readily apparent that in all cases the most favorable interaction corresponds to HOMO (diene)−LUMO (dienophile), as expected for a cycloaddition controlled by *normal electron demand*.[16,17] Furthermore, the energy gap is smaller for both conformers

(16) Fleming, I. *Frontier Orbitals and Organic Chemical Reactions*; Wiley: Chichester, U.K., 1976.

(17) Fernández, I.; Sierra, M. A.; Cossio, F. P. *J. Org. Chem.* **2008**, *73*, 2083–2089.

Table 7. Aromatization of Compound 10b using Various Reaction Conditions

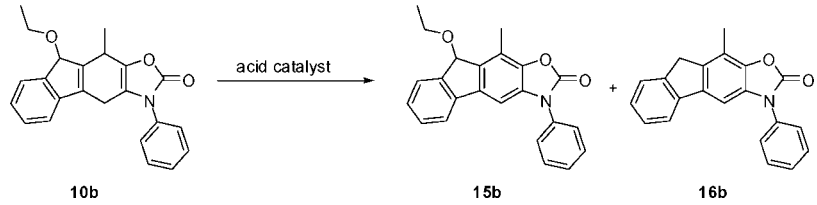

entry	conditions	product	yield (%)
1	SiO_2/*p*-TsOH/$CHCl_3$/room temp, 72 h	**15b/16b**	10/20
2	*p*-TsOH/$CHCl_3$/room temp, 72 h	**15b/16b**	5/13
3	SiO_2/*p*-TsOH/THF/reflux, 12 h	**15b/16b**	10/53
4	SiO_2/HCl/toluene/reflux, 3 h	**16b**	65

Table 8. General Method for the Aromatization of Fluorenyloxazol-2-(4*H*,9*H*,10*H*)-ones 10b−f

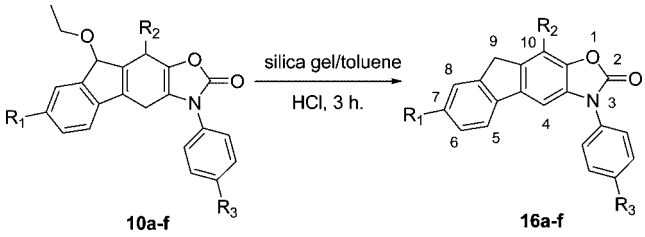

entry	R_1	R_2	R_3	product	yield (%)
1	H	H	H	**16a**	85
2	H	CH_3	H	**16b**	60
3	H	CH_3CH_2	H	**16c**	55
4	H	CH_3	Cl	**16d**	50
5	CH_3	CH_3	H	**16e**	55
6	CH_3O	CH_3	H	**16f**	55

Table 9. Aromatization Reactions of 10a−f with DDQ

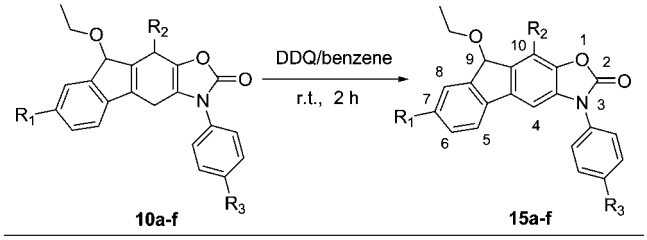

entry	R_1	R_2	R_3	product	yield (%)
1	H	H	H	**15a**	85
2	H	CH_3	H	**15b**	80
3	H	CH_3CH_2	H	**15c**	75
4	H	CH_3	Cl	**15d**	80
5	CH_3	CH_3	H	**15e**	90
6	CH_3O	CH_3	H	**15f**	85

of carbenes **1** than for **14**, a fact which suggests that these former carbenes should be more reactive than the latter, in agreement with experimental results.[7b] In all cases, the energy gaps are smaller for the anti conformers, reflecting the higher stability of their LUMO (Table 4).

Table 5 also shows the difference between both possible HOMO−LUMO energy gaps ($\Delta\Delta E$). These values are larger for the carbene complexes than for the ester, predicting a higher selectivity in the cycloadditions to the carbenes in comparison with the metal-free dienophiles.[17] These FMO calculations are in parallel with recent ground-state and transition-state calculations of alkenylchromium and -tungsten carbenes.[17]

The regioselectivity can be analyzed in terms of the atomic orbital coefficients of the molecular orbitals corresponding to the dominant MO interactions, which for these reactions are summarized in Table 6.

The coefficient values in Table 6 predict the *para* regioselectivity in all cases, as observed in the actual reactions. The difference in coefficients (Δc) in the dienophiles is much larger for the carbenes, **1a**,**d**, than for the ester, **14**; thus, a higher regioselectivity is expected for the carbenes. An additional observation is that the Δc value is slightly larger for tungsten than for chromium.

These calculations indicate that carbene **1d** should be more reactive than carbene **1a**, in agreement with previous kinetic measurements.[9] However, they do not correspond with the results shown in Table 2. It is likely that other effects are involved in our cycloadditions to afford an inverse reactivity, apart from electronic effects, which are mostly related to FMO interactions, such as chemical stability of carbenes (vide supra). Moreover, steric hindrance due to the presence of alkyl substituents (methyl or ethyl groups) in the diene moiety has been revealed as a factor in modifying reactivity in Diels−Alder reactions.[7e,18] Hence, owing to its larger size, the tungsten carbene **1d** could generate stronger steric interactions than carbene **1a** when approaching the diene at the transition state.

Aromatization of 9-Ethoxy-3-phenyl-3*H*-fluorene[3,2-*d*]oxazol-2-(4*H*,9*H*,10*H*)-ones 10a−f. The tandem [4 + 2] cycloaddition/cyclopentannulation reactions proved to be an efficient process for building the 9-ethoxy-3-phenyl-3*H*-fluorene[3,2-*d*]oxazol-2-(4*H*,9*H*,10*H*)-one scaffold. Fluorenyloxazolones **10a−f** possess a 1,4-cyclohexadiene core, which may be expected to undergo an efficient aromatization reaction.

In the course of the current study, an initial attempt was made to isolate **10a** via column chromatography rather than crystallization. We found that the 1,3-cyclohexadiene nucleus of **10a** in *n*-hexane/AcOEt was aromatized to give the 9-ethoxyfluorenyloxazol-2-(9*H*)-one compound **15a** upon being exposed either to silica gel for a long time or to a $CDCl_3$ solution (Scheme 6).

Compound **15a** was isolated as a single product and, like its precursor, had 20 signals in the proton-decoupled ^{13}C NMR spectrum. Its ^1H NMR spectrum possessed a benzylic/benzylic proton H-9 at 5.61 ppm, as opposed to the benzylic/allylic proton H-9 observed at 5.07 ppm for **10a**. Furthermore, the infrared spectrum of **15a** displayed a carbonyl absorption at 1773 cm^{-1}, in contrast to the carbonyl absorptions at 1763 and 1714 cm^{-1} for **10a**.

However, fluorenyloxazol-2-(4*H*,9*H*,10*H*)-ones **10b−f** were found to be stable under similar conditions. Their attempted aromatization on silica gel with $CHCl_3$ led only to recovery of the starting material. In order to favor the aromatization of

(18) Martínez, R.; Jiménez-Vázquez, H. A.; Reyes, A.; Tamariz, J. *Helv. Chim. Acta* **2002**, *85*, 464–482.

10b−f, the adduct **10b** was reacted with silica gel and *p*-toluenesulfonic acid in $CHCl_3$ as the solvent at room temperature for 72 h to give a mixture of **15b** (10%) and **16b** (20%) in low yields, the latter with the loss of the ethoxy group at position C-9 (Table 7, entry 1).

After screening several reaction conditions (Table 7, entries 2 and 3), we found that the best results, in terms of yields and selectivity to carry out the transformation of **10b** to **16b**, were obtained in the presence of silica gel and a catalytic amount of concentrated HCl, after refluxing in toluene for 3 h. Thus, fluorenyloxazol-2-(9*H*)-one **16b** was obtained in a fair yield (65%) (Table 7, entry 4), judging from the ^{1}H NMR (300 MHz) analysis of the crude reaction mixture.

These results show that the acid catalyst employed can control the formation of the products. In particular, hydrochloric acid seems to play a key role in favoring the loss of the ethoxy group in **10b** and preventing the formation of compound **15b**, leading to the exclusive formation of compound **16b**.

In order to investigate the scope and limitations of this aromatization reaction, as well as to identify the possible effect induced by other substrates on the formation of compounds **16**, we carried out the reaction with substrates **10a**,**c−f** under the same reaction conditions. A similar behavior was observed with respect to **10b**, leading to adducts **16a**,**c−f** as single products in comparable yields (Table 8).

Compounds **16a−f** were isolated as solids, and their ^{1}H and ^{13}C NMR spectra were consistent with the fluorenyloxazol-2(9*H*)-one skeleton. In addition, they did not show the presence of the ethoxy group at C-9 and the methylene and methine groups at C-4 and C-10, respectively. Instead, the signals of a methylene group at 3.77−3.85 ppm (H-9) and an aromatic proton (H-4 and H-10) appeared in the range 7.16−7.55 ppm. The molecular structures of **16b**,**e** were confirmed by single-crystal X-ray analysis (Figures 6 and 7).

The determination that the use of a protic acid involves an aromatization reaction with the removal of the ethoxy group in C-9 of **10** prompted us to consider the formation of **15** in a neutral medium. The aromatization of the series of analogues **10a−f** to **15a−f** was carried out with DDQ in benzene at room temperature for 2 h, affording the desired compounds **15a−f** in high yields (75−90%, Table 9).

The structures of compounds **15a−f** were assigned on the basis of their 1D and 2D NMR spectral data (^{1}H, ^{13}C, COSY, HMQC, and HMBC experiments) and HRMS. Their ^{1}H and ^{13}C NMR spectra are consistent with the 9-ethoxyfluorenyloxazol-2(9*H*)-one skeleton, showing the presence of the ethoxy group at C-9 (^{1}H NMR 5.60−5.74 ppm (H-9), 2.95−3.27 ppm (OCH_2CH_3), 1.13−1.40 ppm (OCH_2CH_3); ^{13}C NMR 79.8−80.5 ppm (C-9), 59.0−60.5 ppm (OCH_2CH_3), 15.4−15.8 ppm (OCH_2CH_3)) and the methine group at C-4 (^{1}H NMR 7.04−7.36 ppm (H-4); ^{13}C NMR 97.7−100.9 ppm).

The new oxazol-2-one compounds obtained in this work (**10**, **13**, **15**, and **16**) are themselves potential biologically active compounds[19] and precursors in organometallic and organic synthesis. For example, the oxazolone group can be a useful synthon to form diarylamines, which may be efficiently transformed into carbazoles.[8]

(19) (a) Weinstock, J.; Gaitanopoulos, D. E.; Stringer, O. D.; Franz, R. G.; Hieble, J. P.; Lewis, B.; Kinter, L. B.; Mann, W. A.; Flaim, K. E.; Gessners, G. *J. Med. Chem.* **1987**, *30*, 1167–1176. (b) Ceccarelli, S. M.; Jaeschke, G.; Buettelmann, B.; Huwyler, J.; Kolczewski, S.; Peters, J. U.; Prinssen, E.; Porter, R.; Spooren, W.; Vieira, E. *Bioorg. Med. Chem. Lett.* **2007**, *17*, 1302–1306. (c) Erol, D. D.; Aytemir, M. D.; Yulug, N. *Eur. J. Med. Chem.* **1996**, *31*, 731–734.

Conclusions

The tandem [4 + 2] cycloaddition/cyclopentannulation/1,5-sigmatropic rearrangement reactions of Fischer (arylethynyl)(ethoxy)carbene complexes **1a−f** with *exo*-2-oxazolidinone dienes **7a−d** constitute a general regio- and stereocontrolled method for the synthesis of a variety of novel substituted fluorenyl[3,2-*d*]oxazol-2-(4*H*,9*H*,10*H*)-ones, **10a−f**. Furthermore, the Diels−Alder reaction between carbene complex **12** and diene **7b** to afford the carbene adduct **13** corroborates the high *para* regioselectivity in these cycloadditions and supports the proposed mechanism, in which the unstable complex **I** is suggested as the precursor in the tandem process. The reactivity and regioselectivity of these cycloadditions were rationalized by DFT calculations of geometries as well as FMO energies and coefficients of complexes **1a**,**d** and diene **7a**. In addition, the adducts **10a−f** can be selectively converted into the corresponding 9-ethoxyfluorenyl[3,2-*d*]oxazol-2-(9*H*)-ones **15a−f** or the fluorenyloxazol-2-(9*H*)-ones **16a−f** through an aromatization reaction under mild conditions.

Experimental Section

All reactions were carried out under nitrogen in anhydrous solvents. All glassware was dried in an oven prior to use. All commercially available compounds were used without further purification. Tetrahydrofuran (THF) was distilled from sodium benzophenone ketyl under a N_2 atmosphere prior to use. *n*-Hexane and ethyl acetate were distilled before use. Melting points (uncorrected) were determined with a Fisher-Johns melting point apparatus. ^{1}H NMR and ^{13}C NMR spectra were recorded on a Varian Mercury (300 MHz) instrument, in $CDCl_3$ as solvent and with TMS as internal reference. High-resolution mass spectra (HRMS) were obtained with a JSM-GCMate II mass spectrometer, and electron impact techniques (70 eV) were employed. X-ray data were collected on Siemens P4 and Oxford Diffraction Xcalibur S single-crystal X-ray diffractometers. TLC analyses were performed using silica plates and were visualized using UV (254 nm) or iodine. The chromium and tungsten carbene complexes **1a−f**,[4c] **12**,[11] and the *exo*-2-oxazolidinone dienes **7a−d**[7] were prepared by the methods described in the literature.

General Procedure for the Tandem Reaction of Complexes 1a−f with *exo*-2-Oxazolidinone Dienes 7a−d. A solution of the corresponding complexes **1** (0.33 mmol) and dienes **7** (0.33 mmol) in 10 mL of dry THF was stirred at 50 °C. After 6−13 h, the solvent was removed under reduced pressure. The residue was purified by column chromatography on silica gel using *n*-hexane/EtOAc (98:2) as eluent, to afford the corresponding cycloadducts **10a−f**.

(9*R)-9-Ethoxy-3-phenyl-3*H*-fluorene[3,2-*d*]oxazol-2-(4*H*,9*H*,10*H*)-one (10a).** Yield: 40% (yellow solid, mp 186−187 °C). FT-IR: ν_{max} 1763 (C═O), 1714 (C═C) cm^{-1}. ^{1}H NMR (300 MHz, $CDCl_3$): δ 1.20 (t, J = 6.9 Hz, 3H, OCH_2CH_3), 3.28−3.40 (m, 4H, H-4, OCH_2CH_3), 3.47−3.55 (m, 2H, H-10), 5.07 (s, 1H, H-9), 7.10 (d, J = 6.6 Hz, 1H, H-5), 7.29−7.40 (m, 2H, H-6, H-7), 7.42−7.55 (m, 6H, H-8, H-12, H-13, H-14). ^{13}C NMR (75.4 MHz, $CDCl_3$): δ 15.6 (OCH_2CH_3), 21.0 (C-4), 22.6 (C-10), 60.9 (OCH_2CH_3), 82.7 (C-9), 118.3 (C-3a), 118.7 (C-5), 123.8 (C-8), 125.2 (C-12), 125.9 (C-6), 128.4 (C-7), 128.6 (C-14), 129.6 (C-13), 133.4 (C-4a), 133.9 (C-11), 137.4 (C-10a), 141.9 (C-4b), 142.3 (C-9a), 143.8 (C-8a), 155.2 (C-2). EIMS (70 eV; *m*/*z* (%)): 345 (25) 316 (15), 299 (100), 254 (15), 197 (10). HRMS (EI): *m*/*z* calcd for $C_{22}H_{19}NO_3$ 345.1365, found 345.1366.

(9*S,10*R**)-9-Ethoxy-10-methyl-3-phenyl-3*H*-fluorene[3,2-*d*]oxazol-2-(4*H*,9*H*,10*H*)-one (10b).** Yield: 45% (yellow solid, mp 189−190 °C). FT-IR: ν_{max} 1761 (C═O), 1715 (C═C) cm^{-1}. ^{1}H NMR (300 MHz, $CDCl_3$): δ 1.19 (t, J = 7.0 Hz, 3H, OCH_2CH_3),

1.53 (d, $J = 7.0$ Hz, 3H, CH_3), 3.22−3.40 (m, 4H, H-4, OCH_2CH_3), 3.68−3.78 (m, 1H, H-10), 5.20 (s, 1H, H-9), 7.10 (d, $J = 6.6$ Hz, 1H, H-5), 7.22−7.29 (m, 2H, H-6, H-7), 7.42−7.44 (m, 3H, H-12, H-14), 7.51−7.54 (m, 3H, H-8, H-13). ^{13}C NMR (75.4 MHz, $CDCl_3$): δ 15.9 (OCH_2CH_3), 19.1 (CH_3), 21.3 (C-4), 27.9 (C-10), 61.1 (OCH_2CH_3), 80.7 (C-9), 118.2 (C-3a), 118.7 (C-5), 124.0 (C-8), 125.2 (C-12), 126.3 (C-6), 128.6 (C-14), 128.7 (C-7), 129.8 (C-13), 133.0 (C-4a), 134.2 (C-11), 138.1 (C-10a), 142.8 (C-4b), 142.6 (C-9a), 143.1 (C-8a), 155.1 (C-2). EIMS (70 eV; *m*/*z* (%)): 359 (65), 344 (20), 313 (100), 298 (60), 268 (10), 254 (15), 218 (25). HRMS (EI): *m*/*z* calcd for $C_{23}H_{21}NO_3$ 359.1521, found 359.1518.

(9*S,10*R**)-9-Ethoxy-10-ethyl-3-phenyl-3*H*-fluorene[3,2-*d*]oxazol-2-(4*H*,9*H*,10*H*)-one (10c).** Yield: 70% (yellow solid, mp 196−197 °C). FT-IR: ν_{max} 1762 (C═O), 1710 (C═C) cm^{-1}. ^{1}H NMR (300 MHz, $CDCl_3$): δ 0.86 (t, $J = 7.5$ Hz, 3H, CH_2CH_3), 1.18 (t, $J = 7.0$ Hz, 3H, OCH_2CH_3), 1.90−1.94 (m, 1H, CH_2CH_3), 2.07−2.10 (m, 1H, CH_2CH_3), 3.23−3.40 (m, 4H, OCH_2CH_3, H-4), 3.74−3.82 (m, 1H, H-10), 5.18 (s, 1H, H-9), 7.10 (dd, $J = 6.6$, 0.9 Hz, 1H, H-5), 7.20−7.23 (m, 2H, H-6, H-7), 7.52−7.55 (m, 3H, H-12, H-14), 7.52−7.55 (m, 3H, H-8, H-13). ^{13}C NMR (75.4 MHz, $CDCl_3$): δ 9.4 (CH_2CH_3), 15.6 (OCH_2CH_3), 21.1 (C-4), 24.5 (C-10), 33.7 (CH_2CH_3), 60.7 (OCH_2CH_3), 80.4 (C-9), 118.3 (C-5), 119.4 (C-3a), 123.9 (C-8), 125.8 (C-6), 125.5 (C-12), 127.9 (C-14), 128.4 (C-7), 129.5 (C-13), 133.9 (C-4a), 134.4 (C-11), 136.1 (C-10a), 141.1 (C-4b), 141.9 (C-9a), 142.4 (C-8a), 154.8 (C-2). HRMS (EI): *m*/*z* calcd for $C_{24}H_{23}NO_3$ 373.1670, found 373.1678.

(9*S,10*R**)-3-(4-Chlorophenyl)-9-ethoxy-10-methyl-3*H*-fluorene[3,2-*d*]oxazol-2-(4*H*,9*H*,10*H*)-one (10d).** Yield: 60% (yellow solid, mp 189−190 °C). FT-IR: ν_{max} 1757 (C═O), 1712 (C═C) cm^{-1};. ^{1}H NMR (300 MHz, $CDCl_3$): δ 1.25 (t, $J = 7.2$ Hz, 3H, OCH_2CH_3), 1.50 (d, $J = 6.9$ Hz, 3H, CH_3), 3.25−3.40 (m, 4H, H-4, OCH_2CH_3), 3.68−377 (m, 1H, H-10), 5.20 (s, 1H, H-9), 7.10 (d, $J = 7.2$ Hz, 1H, H-5), 7.20−7.23 (m, 2H, H-6, H-7), 7.39 (dd, $J = 9$ Hz, 2.1 Hz, 2H, H-12), 7.51 (dd, $J = 9$ Hz, 2H, H-13); 7.53 (s, 1H, H-8). ^{13}C NMR (75.4 MHz, $CDCl_3$): δ 15.6 (OCH_2CH_3), 18.6 (CH_3), 21.0 (C-4), 28.0 (C-10), 60.9 (OCH_2CH_3), 80.4 (C-9), 117.6 (C-3a), 118.4 (C-5), 123.9 (C-8), 126.0 (C-6), 126.7 (C-12), 128.4 (C-14), 128.5 (C-7), 129.8 (C-13), 132.5 (C-4a), 133.8 (C-11), 138.2 (C-10a), 141.9 (C-4b), 142.3 (C-9a), 142.5 (C-8a), 154.5 (C-2). HRMS (EI): *m*/*z* calcd for $C_{23}H_{20}ClNO_3$ 393.1131, found 393.1134.

(9*S,10*R**)-9-Ethoxy-7,10-dimethyl-3-phenyl-3*H*-fluorene[3,2-*d*]oxazol-2-(4*H*,9*H*,10*H*)-one (10e).** Yield: 65% (yellow solid, mp 194−195 °C). FT-IR: ν_{max} 1759 (C═O), 1710 (C═C) cm^{-1}. ^{1}H NMR (300 MHz, $CDCl_3$): δ 1.19 (t, $J = 6.9$ Hz, 3H, OCH_2CH_3), 1.52 (d, $J = 7.0$ Hz, 3H, CH_3), 2.38 (s, 3H, Ar−CH_3), 3.24−3.40 (m, 4H, OCH_2CH_3, H-4), 3.64−3.76 (m, 1H, H-10), 5.20 (s, 1H, H-9), 6.98 (d, $J = 7.5$ Hz, 1H, H-5), 7.10 (d, $J = 7.5$ Hz, 1H, H-6), 7.34 (s, 1H, H-8), 7.41−7.55 (m, 5H, H-12, H-13, H-14). ^{13}C NMR (75.4 MHz, $CDCl_3$): δ 15.7 (OCH_2CH_3), 18.7 (CH_3), 21.2 (C-4), 21.4 (Ar−CH_3), 27.9 (C-10), 60.5 (OCH_2CH_3), 80.3 (C-9), 117.9 (C-3a), 118.1 (C-5), 124.9 (C-8), 125.6 (C-12), 128.0 (C-14), 128.9 (C-6), 129.6 (C-13), 132.6 (C-4a), 133.9 (C-11), 135.8 (C-7), 137.9 (C-9a), 139.4 (C-4b), 141.7 (C-10a), 142.5 (C-8a), 154.8 (C-2). HRMS (EI): *m*/*z* calcd for $C_{24}H_{23}NO_3$ 373.1678, found 373.1684.

(9*S,10*R**)-9-Ethoxy-7-methoxy-10-methyl-3-phenyl-3*H*-fluorene[3,2-*d*]oxazol-2-(4*H*,9*H*,10*H*)-one (10f).** Yield: 60% (yellow solid, mp 186−187 °C). FT-IR: ν_{max} 1765 (C═O), 1712 (C═C) cm^{-1}. ^{1}H NMR (300 MHz, $CDCl_3$): δ 1.20 (t, $J = 7.8$ Hz, 3H, OCH_2CH_3), 1.52 (d, $J = 7.8$ Hz, 3H, CH_3), 3.23−3.45 (m, 4H, OCH_2CH_3, H-4), 3.62−3.74 (m, 1H, H-10), 3.80 (s, 3H, Ar−OCH_3), 5.20 (s, 1H, H-9), 6.79 (dd, $J = 8.1$, 2.1 Hz, 1H, H-6), 7.00 (d, $J = 8.1$ Hz, 1H, H-5), 7.12 (d, $J = 2.1$ Hz, 1H, H-8), 7.26−7.43 (m, 3H, H-12, H-14), 7.49−7.55 (m, 2H, H-13). ^{13}C NMR (75.4 MHz, $CDCl_3$): δ 15.6 (OCH_2CH_3), 18.7 (CH_3), 21.1 (C-4), 27.9 (C-10), 55.5 (Ar−OCH_3), 60.5 (OCH_2CH_3), 80.3 (C-9), 111.4 (C-8), 112.7 (C-6), 117.9 (C-3a), 118.8 (C-5), 125.6 (C-12), 128.0 (C-14), 129.6 (C-13), 132.5 (C-4a), 133.9 (C-11), 134.9 (C-10a), 137.9 (C-9a), 140.5 (C-4b), 144.2 (C-8a), 154.8 (C-2), 158.7 (C-7);. HRMS (EI): *m*/*z* calcd for $C_{24}H_{23}NO_4$ 389.1671, found 389.1621.

{(5-Propyl-7-methyl-2-oxo-3-phenyl-2,3,4,7-tetrahydrobenzo-[*d*]oxazole-6-ethoxymethylene)}pentacarbonyltungsten (13). Yield: 55% (orange solid, mp 124−125 °C). FT-IR: ν_{max} 2068, 1944, (WCO), 1767 (C═O) cm^{-1}. ^{1}H NMR (300 MHz, $CDCl_3$): δ 0.87 (t, $J = 14.1$ Hz, 3H, H-14), 1.11 (d, $J = 6.9$ Hz, 3H, H-15), 1.43−1.45 (m, 2H, H-13), 1.67 (t, $J = 14.1$ Hz 3H, OCH_2CH_3), 1.85−1.88 (m, 2H, H-12), 3.00 (d, $J = 6.9$ Hz, 2H, H-4), 4.07−4.13 (m, 1H, H-7), 4.94−4.96 (m, 2H, OCH_2CH_3), 7.36−7.39 (m, 3H, H-9, H-11), 7.45−7.48 (m, 2H, H-10). ^{13}C NMR (75.4 MHz, $CDCl_3$): δ 14.3 (C-14), 15.1 (OCH_2CH_3), 17.9 (C-15), 21.6 (C-13), 25.8 (C-4), 31.8 (C-7), 36.2 (C-12), 80.4 (OCH_2CH_3), 117.3 (C-3a), 121.3 (C-6), 125.1 (C-9), 127.8 (C-11), 129.4 (C-10), 133.8 (C-8), 135.1 (C-7a), 150.9 (C-5), 154.7 (C-2), 196.8 (CO cis), 202.8 (CO *trans*), 331.8 (W═C). HRMS (EI): *m*/*z* calcd for $C_{26}H_{25}NO_8W$ 649.0933, found 649.1006.

General Procedure To Obtain the Compounds 15a−f. A solution of the corresponding **10a-f** (0.30 mmol) and DDQ (0.36 mmol) in 10 mL of dry benzene was stirred at room temperature. After 2 h, the solvent was removed under reduced pressure. The residue was purified by column chromatography on silica gel using *n*-hexane/EtOAc (99:1) as eluent, obtaining the corresponding products **15a-f.**

(9*S)-9-Ethoxy-3-phenyl-3*H*-fluoreno[3,2-*d*]oxazol-2(9*H*)-one (15a).** Yield: 85% (white solid, mp 144−145 °C). FT-IR: ν_{max} 1773 (C═O) cm^{-1}. ^{1}H NMR (300 MHz, $CDCl_3$): δ 1.17 (t, $J = 7.2$ Hz, 3H, OCH_2CH_3), 3.27 (q, $J = 7.2$, Hz, 2H, OCH_2CH_3), 5.61 (s, 1H, H-9), 7.25−7.36 (m, 3H, H-4, H-6, H-7), 7.47−7.53 (m, 3H, H-5, H-10, H-14), 7.60−7.61 (m, 5H, H-8, H-12, H-13). ^{13}C NMR (75.4 MHz, $CDCl_3$): δ 15.6 (OCH_2CH_3), 60.5 (OCH_2CH_3), 80.5 (C-9), 100.9 (C-4), 108.0 (C-10), 119.5 (C-5), 125.2 (C-12), 125.3 (C-8), 127.4 (C-6), 128.5 (C-7), 129.0 (C-14), 129.9 (C-13), 131.9 (C-4a), 133.4 (C-10a), 136.9 (C-3a), 138.7 (C-11), 139.8 (C-4b), 142.4 (C-9a), 143.2 (C-8a), 153.3 (C-2). HRMS (EI): *m*/*z* calcd for $C_{22}H_{17}NO_3$ 343.1208, found 343.1189.

(9*S)-9-Ethoxy-10-methyl-3-phenyl-3*H*-fluoreno[3,2-*d*]oxazol-2(9*H*)-one (15b).** Yield: 80% (white solid, mp 204−205 °C). FT-IR: ν_{max} 1770 (C═O) cm^{-1}. ^{1}H NMR (300 MHz, $CDCl_3$): δ 1.13 (t, $J = 7.2$ Hz, 3H, OCH_2CH_3), 2.59 (s, 3H, CH_3), 3.09−3.17 (m, 2H, OCH_2CH_3), 5.71 (s, 1H, H-9), 7.14 (s, 1H, H-4), 7.26−7.38 (m, 2H, H-6, H-7), 7.46−7.54 (m, 2H, H-5, H-14), 7.57−7.61 (m, 5H, H-8, H-12, H-13). ^{13}C NMR (75.4 MHz, $CDCl_3$): δ 10.9 (CH_3), 15.6 (OCH_2CH_3), 59.2 (OCH_2CH_3), 80.0 (C-9), 98.4 (C-4), 119.4 (C-5), 120.0 (C-4a), 125.1 (C-8), 125.2 (C-12), 127.2 (C-6), 128.4 (C-14), 128.9 (C-7), 129.8 (C-13), 131.6 (C-3a), 133.5 (C-11), 136.5 (C-10), 136.7 (C-9a), 140.2 (C-4b), 141.2 (C-10a), 143.0 (C-8a), 153.5 (C-2). HRMS (EI): *m*/*z* calcd for $C_{23}H_{19}NO_3$ 357.1364, found 357.1365.

(9*S)-9-Ethoxy-10-ethyl-3-phenyl-3*H*-fluoreno[3,2-*d*]oxazol-2(9*H*)-one (15c).** Yield: 75% (white solid, mp 160−161 °C). FT-IR: ν_{max} 1773 (C═O) cm^{-1}. ^{1}H NMR (300 MHz, $CDCl_3$): δ 1.13 (t, $J = 7.2$ Hz, 3H, CH_2CH_3), 1.40 (t, $J = 7.2$ Hz, 3H, OCH_2CH_3), 2.95−3.25 (m, 4H, CH_2CH_3, OCH_2CH_3), 5.74 (s, 1H, H-9), 7.15 (s, 1H, H-4), 7.25−7.37 (m, 2H, H-6, H-7), 7.46−7.53 (m, 2H, H-5, H-14), 7.59−7.60 (m, 5H, H-8, H-12, H-13). ^{13}C NMR (75.4 MHz, $CDCl_3$): δ 13.6 (CH_2CH_3), 15.4 (OCH_2CH_3), 19.5 (CH_2CH_3), 59.2 (OCH_2CH_3), 79.8 (C-9), 98.6 (C-4), 119.3 (C-5), 125.1 (C-8), 125.2 (C-12), 126.3 (C-10), 127.2 (C-6), 128.4 (C-14), 128.9

(C-7), 129.8 (C-13), 131.8 (C-4a), 133.5 (C-11), 135.7 (C-9a), 136.9 (C-3a), 140.2 (C-8a), 140.9 (C-10a), 142.9 (C-4b), 153.5 (C-2). HRMS (EI): *m/z* calcd for $C_{24}H_{21}NO_3$ 371.1521, found 371.1504.

(9*S)-3-(4-Chlorophenyl)-9-ethoxy-10-methyl-3*H*-fluoreno[3,2-*d*]oxazol-2(9*H*)-one (15d).** Yield: 80% (white solid, mp 219−220 °C). FT-IR: ν_{max} 1774 (C═O) cm^{-1}. ^1H NMR (300 MHz, $CDCl_3$): δ 1.13 (t, J = 7.2 Hz, 3H, OCH_2CH_3), 2.58 (s, 3H, CH_3), 3.12 (q, J = 7.2, 6.9 Hz, 2H, OCH_2CH_3), 5.70 (s, 1H, H-9), 7.12 (s, 1H, H-4), 7.26−7.39 (m, 2H, H-6, H-7), 7.52−7.62 (m, 6H, H-5, H-8, H-12, H-13). ^{13}C NMR (75.4 MHz, $CDCl_3$): δ 10.9 (CH_3), 15.5 (OCH_2CH_3), 59.3 (OCH_2CH_3), 80.0 (C-9), 98.2 (C-4), 119.4 (C-5), 120.2 (C-4a), 125.2 (C-8), 126.4 (C-12), 127.3 (C-6), 129.0 (C-7), 130.0 (C-13), 131.2 (C-3a), 132.0 (C-11), 134.1 (C-10), 136.7 (C-9a), 136.8 (C-4b), 140.0 (C-10a), 141.1 (C-14), 143.0 (C-8a), 153.2 (C-2). HRMS (EI): *m/z* calcd for $C_{23}H_{18}ClNO_3$ 391.0975, found 391.0979.

(9*S)-9-Ethoxy-7,10-dimethyl-3-phenyl-3*H*-fluoreno[3,2-*d*]oxazol-2(9*H*)-one (15e).** Yield: 90% (yellow solid, mp 219−220 °C). FT-IR: ν_{max} 1771 (C═O) cm^{-1}. ^1H NMR (300 MHz, $CDCl_3$): δ 1.13 (t, J = 7.2 Hz, 3H, OCH_2CH_3), 2.41 (s, 3H, Ar−CH_3), 2.57 (s, 3H, CH_3), 3.15 (q, J = 7.2, 2H, OCH_2CH_3), 5.60 (s, 1H, H-9), 7.10 (s, 1H, H-4), 7.17 (d, J = 8.4 Hz, 1H, H-6), 7.40−7.42 (m, 2H, H-5, H-8), 7.46−7.50 (m, 1H, H-14), 7.58−7.61 (m, 4H, H-12, H-13). ^{13}C NMR (75.4 MHz, $CDCl_3$): δ 11.2 (CH_3), 15.8 (OCH_2CH_3), 21.8 (Ar−CH_3), 59.4 (OCH_2CH_3), 80.2 (C-9), 98.4 (C-4), 119.4 (C-5), 120.2 (C-4a), 125.5 (C-12), 126.1 (C-8), 128.6 (C-6), 129.9 (C-14), 130.1 (C-13), 131.8 (C-3a), 133.8 (C-11), 136.5 (C-9a), 137.1 (C-10), 137.5 (C-7), 137.8 (C-4b), 141.1 (C-10a), 143.5 (C-8a), 153.8 (C-2). HRMS (EI): *m/z* calcd for $C_{24}H_{21}NO_3$ 371.1521, found 371.1523.

(9*S)-9-Ethoxy-7-methoxy-10-methyl-3-phenyl-3*H*-fluoreno[3,2-*d*]oxazol-2(9*H*)-one (15f).** Yield: 85% (yellow solid, mp 177−178 °C). FT-IR: ν_{max} 1770 (C═O) cm^{-1}. ^1H NMR (300 MHz, $CDCl_3$): δ 1.13 (t, J = 7.2 Hz, 3H, OCH_2CH_3), 2.56 (s, 3H, CH_3), 3.10 (q, J = 7.2, 2H, OCH_2CH_3), 3.86 (s, 3H, OCH_3), 5.65 (s, 1H, H-9), 6.88 (dd, J = 2.4, 5.7 Hz, 1H, H-6), 7.04 (s, 1H, H-4), 7.16 (s, 1H, H-8), 7.41−7.51 (m, 2H, H-5, H-14), 7.58−7.60 (m, 4H, H-12, H-13). ^{13}C NMR (75.4 MHz, $CDCl_3$): δ 10.9 (CH_3), 15.5 (OCH_2CH_3), 55.5 (OCH_3), 59.0 (OCH_2CH_3), 79.9 (C-9), 97.7 (C-4), 110.9 (C-8), 114.5 (C-6), 119.9 (C-9a), 120.2 (C-5), 125.2 (C-12), 128.3 (C-14), 129.8 (C-13), 131.6 (C-3a), 133.0 (C-8a), 133.6 (C-11), 135.8 (C-10), 136.8 (C-4a), 140.4 (C-10a), 144.9 (C-4b), 153.5 (C-2), 159.7 (C-7). HRMS (EI): *m/z* calcd for $C_{24}H_{21}NO_4$ 387.1467, found 387.1471.

General Procedure To Obtain the Compounds 16a−f. Solutions of the corresponding compounds **10a−f** (0.30 mmol) in 10 mL of dry toluene and HCl/SiO_2 were stirred at reflux for 3 h. The solvent was removed under reduced pressure. The residue was purified by column chromatography on silica gel using *n*-hexane/EtOAc (99:1) as eluent, to afford the corresponding products **16a−f**.

3-Phenyl-3*H*-fluoreno[3,2-*d*]oxazol-2(9*H*)-one (16a). Yield: 85% (yellow solid, mp 215−216 °C). FT-IR: ν_{max} 1772 (C═O) cm^{-1}. ^1H NMR (300 MHz, $CDCl_3$): δ, 3.85 (s, 2H, H-9), 7.20 (s, 1H, H-4), 7.25−7.36 (m, 2H, H-6, H-7), 7.42−7.55 (m, 3H, H-5, H-10, H-14), 7.58−7.68 (m, 5H, H-8, H-12, H-13). ^{13}C NMR (75.4 MHz, $CDCl_3$): δ 36.9 (C-9), 100.7 (C-4), 107.4 (C-9a), 119.4 (C-5), 124.9 (C-8), 125.2 (C-12), 126.6 (C-6), 126.9 (C-14), 128.3 (C-7), 129.8 (C-13), 130.5 (C-10), 133.6 (C-11), 137.7 (C-4b), 138.4 (C-4a), 140.8 (C-3a), 142.1 (C-10a), 143.1 (C-8a), 152.9 (C-2). EIMS (70 eV; *m/z* (%)): 299 (100), 254 (15), 243 (10), 180 (5), 149 (10). HRMS (EI): calcd for $C_{20}H_{13}NO_2$ 299.0946, found 299.0938.

10-Methyl-3-phenyl-3*H*-fluoreno[3,2-*d*]oxazol-2(9*H*)-one (16b). Yield: 60% (white solid, mp 193−194 °C). FT-IR: ν_{max} 1774 (C═O) cm^{-1}. ^1H NMR (300 MHz, $CDCl_3$): δ 2.50 (s, 3H, CH_3), 3.83 (s, 2H, H-9), 7.25−7.37 (m, 2H, H-4, H-6), 7.44−7.47 (m, 2H, H-7, H-14), 7.54−7.67 (m, 6H, H-8, H-5, H-12, H-13). ^{13}C NMR (75.4 MHz, $CDCl_3$): δ 11.9 (CH_3), 35.5 (C-9), 98.4 (C-4), 117.6 (C-9a), 119.5 (C-5), 124.9 (C-8), 125.2 (C-12), 126.4 (C-6), 126.8 (C-14), 128.2 (C-7), 129.8 (C-13), 130.2 (C-10), 133.8 (C-11), 137.0 (C-4b), 137.8 (C-4a), 140.7 (C-3a), 141.3 (C-10a), 142.8 (C-8a), 153.6 (C-2). EIMS (70 eV; *m/z* (%)): 313 (100), 285 (15), 268 (5), 254 (10), 218 (10), 194 (10), 135 (15). HRMS (EI): *m/z* calcd for $C_{21}H_{15}NO_2$ 313.1097, found 313.1102.

10-Ethyl-3-phenyl-3*H*-fluoreno[3,2-*d*]oxazol-2(9*H*)-one (16c). Yield: 55% (yellow solid, mp 155−156 °C). FT-IR: ν_{max} 1773 (C═O) cm^{-1}. ^1H NMR (300 MHz, $CDCl_3$): δ 1.36 (t, J = 7.5 Hz, 3H, CH_2CH_3), 2.94 (q, 2H, J = 7.5 Hz, CH_2CH_3), 3.85 (s, 2H, H-9), 7.24−7.35 (m, 3H, H-4, H-6, H-14), 7.44−7.65 (m, 7H, H-5, H-7, H-8, H-12, H-13). ^{13}C NMR (75.4 MHz, $CDCl_3$): δ 13.5 (CH_2CH_3), 20.7 (CH_2CH_3), 35.1 (C-9), 98.5 (C-4), 119.4 (C-5), 123.9 (C-9a), 124.9 (C-8), 125.1 (C-12), 126.4 (C-6), 126.8 (C-14), 128.2 (C-7), 129.8 (C-13), 130.4 (C-10), 133.7 (C-11), 136.9 (C-4b), 137.3 (C-4a), 140.2 (C-8a), 141.3 (C-10a), 142.8 (C-3a), 153.6 (C-2). HRMS (EI): *m/z* calcd for $C_{22}H_{17}NO_2$ 327.1261, found 327.1259.

3-(4-Chlorophenyl)-10-methyl-3*H*-fluoreno[3,2-*d*]oxazol-2(9*H*)-one (16d). Yield: 50% (white solid, mp 242−243 °C). FT-IR: ν_{max} 1771 (C═O) cm^{-1}. ^1H NMR (300 MHz, $CDCl_3$): δ 2.49 (s, 3H, CH_3), 3.82 (s, 2H, H-9), 7.25 (s, 1H, H-4), 7.27−7.38 (m, 2H, H-6, H-7), 7.55−7.57 (m, 5H, H-8, H-12, H-13), 7.67 (d, J = 6.9 Hz, 1H, H-5). ^{13}C NMR (75.4 MHz, $CDCl_3$): δ 12.2 (CH_3), 35.8 (C-9), 98.5 (C-4), 118.1 (C-9a), 119.7 (C-5), 125.2 (C-8), 126.6 (C-12), 126.8 (C-6), 127.1 (C-7), 130.0 (C-14), 130.2 (C-13), 132.5 (C-10), 134.1 (C-11), 137.4 (C-4b), 138.3 (C-4a), 140.8 (C-3a), 141.4 (C-10a), 143.1 (C-8a), 153.4 (C-2). HRMS (EI): *m/z* calcd for $C_{21}H_{14}ClNO_2$ 347.0713, found 347.0718.

7,10-Dimethyl-3-phenyl-3*H*-fluoreno[3,2-*d*]oxazol-2(9*H*)-one (16e). Yield: 55% (white solid, mp 178−179 °C). FT-IR: ν_{max} 1773 (C═O) cm^{-1}. ^1H NMR (300 MHz, $CDCl_3$): δ 2.40 (s, 3H, CH_3), 2.42 (s, 3H, Ar−CH_3), 3.83 (s, 2H, H-9), 7.11 (d, J = 6.9 Hz, 1H, H-5), 7.19 (s, 1H, H-4), 7.30 (s, 1H, H-8), 7.41−7.48 (m, 1H, H-14), 7.52 (d, J = 6.9 Hz, 1H, H-6), 7.53−7.61 (m, 4H, H-12, H-13). ^{13}C NMR (75.4 MHz, $CDCl_3$): δ 11.6 (CH_3), 21.7 (Ar−CH_3), 35.5 (C-9), 98.3 (C-4), 117.8 (C-9a), 119.4 (C-5), 125.4 (C-12), 125.9 (C-8), 127.9 (C-14), 128.4 (C-6), 130.0 (C-13), 130.3 (C-10), 134.1 (C-11), 136.6 (C-7), 137.3 (C-4a), 137.8 (C-4b), 138.9 (C-8a), 140.6 (C-10a), 143.3 (C-3a), 153.9 (C-2). HRMS (EI): *m/z* calcd for $C_{22}H_{17}NO_2$ 327.1266, found 327.1259.

7-Methoxy-10-methyl-3-phenyl-3*H*-fluoreno[3,2-*d*]oxazol-2(9*H*)-one (16f). Yield: 55% (white solid, mp 188−189 °C). FT-IR: ν_{max} 1774 (C═O) cm^{-1}. ^1H NMR (300 MHz, $CDCl_3$): δ 2.46 (s, 3H, CH_3), 3.77 (s, 2H, H-9), 3.85 (s, 3H, OCH_3), 6.90 (dd, J = 1.8, 6.6 Hz, 1H, H-6), 7.10 (s, 1H, H-8), 7.16 (s, 1H, H-4), 7.46 (d, J = 6.0 Hz, 1H, H-14), 7.52−7.60 (m, 5H, H-5, H-12, H-13). ^{13}C NMR (75.4 MHz, $CDCl_3$): δ 11.9 (CH_3), 35.5 (C-9), 55.5 (O−CH_3), 97.7 (C-4), 110.6 (C-8), 112.9 (C-6), 117.5 (C-9a), 120.1 (C-5), 125.2 (C-12), 128.2 (C-14), 129.7 (C-13), 130.2 (C-10), 133.8 (C-4a), 134.3 (C-4b), 137.0 (C-10a), 139.9 (C-11), 141.7 (C-3a), 144.7 (C-8a), 153.7 (C-2), 159.7 (C-7). HRMS (EI): *m/z* calcd for $C_{22}H_{17}NO_3$ 343.1182, found 343.1208.

Calculation Methods. The calculations were carried out with the *Gaussian 94* program package[12] at the HF/3-21G, HF/6-31G*, and B3LYP/6-31G* levels of theory, for molecules **7a** and **14**. However, for carbenes **1** a combination of basis sets was employed at the same calculation levels (HF and B3LYP): the standard basis sets already mentioned were used for C, H, and O atoms, and for the Cr or W atoms the LanL2DZ basis set was used, along with the LanL2 effective core potential (ECP) to replace the core electrons of these atoms. For all B3LYP calculations an ultrafine integration grid (INT(GRID═99590)) was employed. We only present the results pertaining to the highest level of theory employed (B3LYP/6-31G*). For all

stationary points we carried out the corresponding frequency analysis in order to identify the nature of the stationary points and determine the zero-point energy (ZPE). All the absolute (E_0) and relative (ΔE_0) energies presented here have been corrected by the inclusion of ZPEs. The FMO analysis was carried out with the B3LYP/6-31G* results; the HF/6-31G* orbital energies and coefficients were similar.

Acknowledgment. We thank Dr. Eleuterio Burgueño for the spectrometry measurements. We thank Bruce A. Larsen for reviewing the use of English in this paper. F.D. acknowledges the CONACyT (Grant No. 44038Q) and CGPI/IPN (Grant Nos. 20050297, 20070617, and 20080331) for financial support. L.R. is grateful to the CONACyT for a graduate scholarship (No. 162803). F.O.-J. thanks DGAPA-UNAM for a postdoctoral fellowship awarded. F.D., J.T., and H.J.-V. are fellows of the EDI/IPN and COFAA/IPN programs.

Supporting Information Available: Figures giving ^{1}H and ^{13}C NMR data for **10a**−**f**, **13**, **15a**−**f**, and **16a**−**f** and tables of crystal data, atomic coordinates, bond lengths and angles, and anisotropic parameters for **10b**,**c**,**e** and **16b**,**e**. This material is available free of charge via the Internet at http://pubs.acs.org.

OM8002416